On the origin of the remarkable stability of aqueous foams stabilised by nanoparticles: link with microscopic surface properties

A. Cervantes Martinez,[a] E. Rio,[a] G. Delon,[a] A. Saint-Jalmes,[b] D. Langevin*[a] and B. P. Binks[c]

Received 11th March 2008, Accepted 24th April 2008
First published as an Advance Article on the web 3rd June 2008
DOI: 10.1039/b804177f

We have performed a quantitative study of the coarsening of foams stabilised by partially hydrophobic silica nanoparticles. We have used a variety of techniques: optical and electron microscopy, microfluidics, and multiple light scattering. Using earlier studies of planar particle monolayers, we have been able to correlate the interfacial properties and the macroscopic temporal evolution of the foam. This has shed light on the origin of the absence of coarsening of particle-stabilised foams. Such particle-stabilised foams appear to be the only known foam system where coarsening is inhibited by surface elasticity.

1. Introduction

Aqueous foams are commonly stabilised by surfactants and/or polymers, or even proteins in the case of food foams.[1] Liquid foams are precursors for light and resistant materials, widely used for insulation, packaging, chair cushions, *etc.* In the case of metallic foams for the automotive and space industries, colloidal particles are being used, since surfactants and polymers chemically degrade at the temperature of the foaming process.[2] It has been reported recently that aqueous foams stabilised by nano- and microparticles alone are much more stable than surfactant or polymer-stabilised foams:[3–6] the latter typically collapse after a maximum of a few tens of hours.

There are different destabilisation mechanisms for foams, the two main ones being drainage followed by bubble coalescence, and coarsening. In the first mechanism, after liquid drainage due to gravity and capillarity, the films between bubbles thin and may eventually rupture: this leads to coalescence of neighbouring bubbles and to an increase of the bubble size with time. If the stabilizing agent (surfactant, polymer, particles) is well chosen, the films can be very stable against rupture. A second destabilisation mechanism known as coarsening (also called Ostwald ripening or disproportionation) also leads to bubble growth and ultimately to foam destruction. Coarsening occurs because the gas pressure inside small bubbles is larger than inside large ones and, as a consequence, the gas diffuses through the aqueous films from the small bubbles towards the large ones. The pressure difference between the inside and outside of any bubble is called the Laplace pressure and is due to the curvature of the bubble surface. This pressure is equal to $4\gamma/R$ for a spherical bubble where γ is the air–water surface tension and R is the bubble radius (the bubble surface tension is twice the air–water tension since the liquid film that covers the bubble surface has two air–water boundaries).

[a]*Laboratoire de Physique des Solides, UMR CNRS 8502, Université Paris Sud, 91405, Orsay, France*
[b]*Institut de Physique de Rennes, UMR 6251, Université Rennes 1, Rennes, 35042, France*
[c]*Surfactant & Colloid Group, Department of Chemistry, University of Hull, Hull, HU6 7RX, UK*

It has already been reported that the coarsening of bubbles can be slowed down or even inhibited if particles are used as the stabilizing agent.[4,7–9] Although it was remarked that particle-stabilised foams do not seem to coarsen, no detailed study of bubble growth has been made up to date. One of the difficulties is the controlled production of sufficient amounts of foam, lasting for at least a few hours, a task much more difficult than for surfactant- or polymer-stabilised foams. In the present study, we have used a turbulent mixing device allowing us to achieve this task. We have also developed a flow-focusing device, allowing us to prepare monodisperse foams and to facilitate observations.

2. Materials and methods

We used hydrophobic fumed silica particles (34% of the surface is covered by silanol groups, the rest by dichlorodimethylsilane groups), supplied by Wacker-Chemie, Burghausen. Fumed silica particles are large fractal-like aggregates, with sizes of the order of 200 nm, made of *ca.* 20 nm silica spheres. For the sake of comparison, we also used a surfactant, sodium dodecyl sulfate (SDS), purchased from Sigma (purity >99%). In order to prepare the silica nanoparticle dispersions, we first wetted the powders with absolute ethanol and diluted the mixture with fresh ultra-purified water from a Millipore-Q instrument (resistivity = 18 MΩ cm). We then sonicated the dispersion in order to break the particle aggregates, using an ultrasonic probe (Ultrasonic Processor) operating at 20 kHz and with an amplitude of 70% (of the maximum amplitude) for 1 hour. After this treatment, the dispersions contain 4.5 wt% of ethanol. The ethanol was then removed using centrifugation–washing cycles, except for use with the flow-focusing device, where bubbles could not be produced with pure water dispersions. Control experiments with the turbulence mixer were also performed keeping the small amount of ethanol, and no differences were noted in the foam properties. For the SDS solutions, we used only fresh ultra-purified water, pH = 5.8.

The foams were produced by two different methods, both using nitrogen as gas. We used a set-up based on the flow-focusing technique[10] to produce monodisperse foams of controlled bubble size. This allowed us to study the coarsening of

monodisperse foams with varying liquid fraction. The sample was placed between two microscope glass slides (76 × 26 mm) spaced by 3 mm. We followed the foam evolution with a CCD camera.

The second foam production method is turbulent mixing,[11] which produces a large volume (about 1 L in 3–5 s) of less monodisperse foam with a homogeneous liquid fraction. The mean bubble radius obtained with particle dispersions is 35 μm and with SDS, 50 μm. The produced foam was placed in a cell 30 cm high, 10 cm wide and 2.5 cm thick made of transparent Plexiglass. To prevent drainage we used a rotating cell set-up[12] which allowed us to maintain the liquid fraction of the foam constant. The cell was rotated every 20 s. The foam coarsening was followed by light transmission. In the limit of multiple scattering, at constant liquid fraction, the transmitted intensity depends linearly on the average bubble radius R.[13] We illuminated one side of the cell with a Nd:YAG laser (Coherent Inc., Compass 315 M, 532 nm wavelength, 100 mW output power) and the intensity was measured on the other side with a CCD camera. We used the software provided with the camera to analyse the variation of the transmitted intensity with time.

3. Results

3.1 Coarsening of quasi 2-D foams

We show in Fig. 1 optical images of aqueous foams containing two layers of monodisperse bubbles made with the flow-focusing device. This allowed us to visualise the bubbles and to avoid liquid drainage. The second layer can be seen behind the first one, with the two bubble lattices spontaneously shifting in order to optimize compaction. The top images of Fig. 1 were taken just after formation and the bottom images 3 hours later. The left-hand pictures (a and b) are from a surfactant-stabilised foam, where substantial growth of the bubbles can be seen with time, t. No coalescence events were seen between frames a and b, so the growth can be attributed to coarsening only. The right-hand pictures (c and d) are from a particle-stabilised foam of similar bubble size, showing that no coarsening occurs within the same timescale.

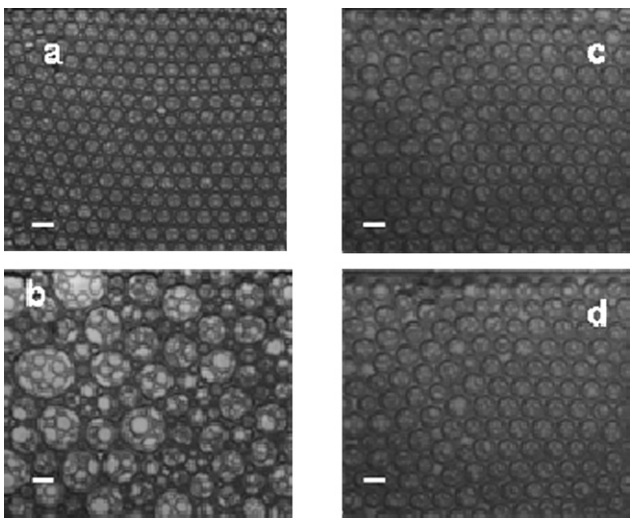

Fig. 1 Snapshots of (left, a and b) SDS (5 wt%)-stabilised aqueous foam and (right, c and d) silica nanoparticle (34% SiOH, 1 wt%)-stabilised foam made with the flow-focusing device. Images a and c correspond to $t = 0$, whilst b and d correspond to 180 minutes. The scale bars correspond to 1 mm.

3.2 Coarsening of 3-D foams

In order to avoid possible influence of the cell walls and to have a truly three-dimensional foam, we used the turbulent mixing method, which allowed us to produce larger amounts of foam than the flow-focusing device. The initial average bubble radius obtained with this instrument is smaller (about 35 μm) and the bubbles are less monodisperse in this case. Since these foams are opaque, we have measured the optical transmission in the multiple light scattering régime, which is proportional to the average bubble radius. We also used a rotating foam cell in order to suppress drainage. Fig. 2 shows the bubble radius *versus* time for surfactant- and particle-stabilised foams. The variation of the average radius is often described by Mullins' expression,[14] valid in the limit of dry foams:

$$R^2(t) = R_0^2[1 + (t - t_0)/\tau] \quad (1)$$

where R_0 is the mean bubble radius at $t = t_0$, which is the time when the experiment is started, and τ is the coarsening time. In the asymptotic limit of long times, a simple scaling is expected, $R \sim t^{1/2}$, which has been reported experimentally.[15] The coarsening time in eqn (1) is given by:[16]

$$\tau = \alpha_v^{2/3} R_0^2/2C \quad (2)$$

where α_v is a geometrical constant: $\alpha_v = V/R^3$, V being the bubble volume; $\alpha_v \sim 4$ in foams. $C = V^{1/3}\mathrm{d}(V^{1/3})/\mathrm{d}t$ is an effective diffusion coefficient constant:[17] $C = 4/3\ K_{gas}\gamma f(\phi)\beta/h$ where K_{gas} is the gas contribution including diffusivity and solubility in water, $f(\phi)$ is a decreasing function of the liquid volume fraction, ϕ accounts for the effective film surface per bubble through which gas transfer occurs, h is the film thickness and β for a given

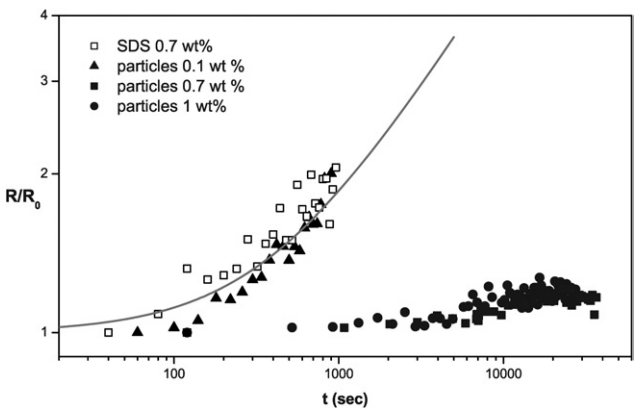

Fig. 2 Normalized average bubble radius *versus* time for SDS- and particle-stabilised foams, the latter made with different bulk particle concentrations, prepared *via* turbulent mixing. The particles are partially hydrophobic silica (34% SiOH). The liquid volume fraction in these foams is 0.25. The characteristic time τ from the fit of the SDS data is 330 s.

bubble is the sum over all its faces of the quantity $HS/V^{1/3}$, H being the film curvature and S its surface area. As a result, coarsening of bubbles turns out to have a strong dependence on the number of faces.[18] In the case of a foam, an effective average curvature must be used: $1/H$ is typically 10 times greater than the bubble radius,[15] and $\beta \sim 1$.

The fit shown in Fig. 2 for the surfactant-stabilised foam (squares) corresponds to a characteristic time τ of 330 s, in agreement with earlier measurements.[12] The film thicknesses calculated using eqn (2) are in the range 20–40 nm, in excellent agreement with the equilibrium thicknesses of freely supported foam films.[19] Let us note however that a fit with eqn (1) and τ constant could not lead to a fully rigorous result, since the initial foams are not fully dry (liquid volume fraction ϕ of 25 %), and the exponent is slightly less than 1/2 (in the régime of dilute bubbles, the scaling is different: $R \sim t^{1/3}$).[19]

Fig. 2 also shows the results for particle-stabilised foams made from dilute particle dispersions (0.1 wt%, triangles), where coarsening is present and is as fast as for the surfactant foam. Because the initial mean bubble radius is smaller (35 μm instead of 50 μm for surfactant foams), the surface tension larger ($\gamma \sim 72$ mN m^{-1},[20] instead of 40 mN m^{-1} for surfactant foams) and the film thickness probably different, the fact that the two curves superimpose is probably a coincidence. In these two cases, the measurements were stopped after 1000 s, because it became difficult to suppress drainage completely (the velocity of which increases with increasing bubble radius).

Foams made with more concentrated particle dispersions ($\geq$ 0.7 wt%) do not coarsen. The slight residual increase observed at much longer times could be due to bubble coalescence (see later). A fit with eqn (1) would give an unrealistically large characteristic time, of the order of 9×10^5 s. According to eqn (2), the main differences between the two types of foams are the film thickness and the surface tension. Since the surface tensions are comparable (of the order of 30 mN m^{-1} for a surface fully covered by particles[20]), in order to account for a time longer by a factor of 3000, the film thickness in the particle foams would need to be much larger than that in surfactant foams. Equilibrium foam films thicknesses for SDS solutions without added salt are of the order of 30 nm; the foam film thickness for particle dispersions would then need to be of the order of 90 μm, *i.e.* larger than the bubble radius.

Fig. 3 shows a photograph of a particle-stabilised foam made with the turbulence mixer and aged 9 months, where one sees that the equilibrium foam films stabilised with particles are much thinner than this estimate. It can be also seen that the foam is quite dry; most of the water has drained out by gravity. However, the films between the bubbles are still present. Some are partly broken (arrow on right), but the network of films is still present. The average bubble radius is around 55 μm, *i.e.* somewhat larger than the initial radius (35 μm). In view of the presence of broken films and of the unrealistic numbers for the coarsening rates, we believe that the small increase in radius (already slightly visible in Fig. 2) is due to bubble coalescence after film rupture.

3.3 Surface coverage

We know from earlier surface pressure studies[20] that for the fumed silica particles that we use, the full particle coverage

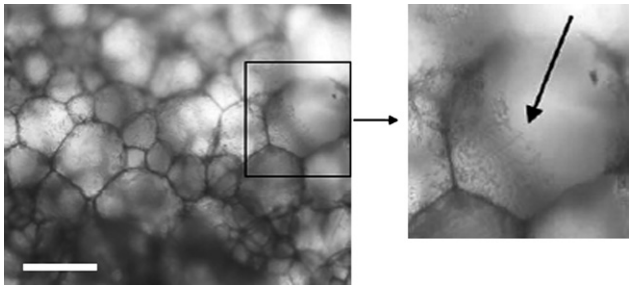

Fig. 3 (Left) Photograph of a silica particle-stabilised foam aged nine months. The foaming dispersion contained 0.6 wt% silica (34% SiOH). The scale bar corresponds to 200 μm. (Right) Enlargement of the portion shown by the black square, showing a partially ruptured film between two bubbles. The intact portion appears rough, the ruptured part smooth, and the limit between the two is irregularly shaped, as expected after the rupture of a fragile film.

corresponds to a surface concentration $\Gamma_{\text{full}} \sim 60$ mg m^{-2}. This may seem high, but it should be noted that fumed silica particles are large fractal-like aggregates, with sizes of the order of 200 nm, made of 20 nm silica spheres. The corresponding monolayers are therefore thick, as indeed evidenced by ellipsometry, hence the large surface concentration.

Cryo-TEM was used to image thin films formed from the dispersion. The film is obtained by placing a drop on a carbon plate of thickness 200 nm and the excess of liquid being removed with a sponge: films of thickness of about 200 nm are thus formed in the pores. The plate is then plunged into liquid ethanol for rapid cooling. Fig. 4(a) shows an image made from a thin film of the aqueous dispersion containing 0.1 wt% particles, where the particles sitting at the film surfaces can be easily seen. This picture also shows that the surface coverage is not complete in this case. Images of films made from a 1 wt% dispersion could not be recorded because of saturation problems. We could, however, image films directly in the foam with an optical microscope: in Fig. 4(b), one sees that the particles are jammed at the bubble surface, as in the case of stable isolated bubbles.[9] The average initial bubble radius in these foams is of the order of 35 μm. If we estimate the surface coverage, we obtain $\Gamma \sim RC/6$, where R is the average bubble radius and C is the bulk particle concentration in the foaming dispersion. For $C = 1$ wt%, we find

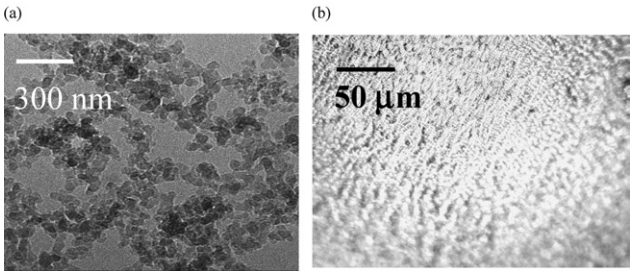

Fig. 4 (a) Cryo-TEM image of a liquid film from the 0.1 wt% silica particle dispersion. The particles are trapped in a glassy water film 200 nm thick. The film thickness being comparable to the particle size, it is likely that these particles bridge both film surfaces. (b) Optical image of the surface of a large bubble made from the 1 wt% dispersion; here one sees that the particles are jammed at the surface.

$\Gamma \sim 60$ mg m^{-2} very close to full coverage, whereas for $C = 0.1$ wt% the surface concentration is only 10% of this value. This confirms that the bubbles of the 1 wt% dispersion are well covered with particles, whereas those of the 0.1 wt% dispersion are not. Furthermore, we have observed for both concentrations that the liquid that drains from the foam is transparent, whereas the initial dispersions are very turbid, confirming that most of the particles are associated with the foam.

4. Discussion

We now have to explain the link between coverage and coarsening. The inhibition of coarsening is sometimes attributed to the fact that particles create a large surface pressure Π at the liquid surface which could decrease the air–water surface tension to zero: $\gamma = \gamma_w - \Pi \sim 0$, where γ_w is the tension in the absence of particles. With zero surface tension, the pressure is the same in all the bubbles of different size and no coarsening could occur. Such a situation can indeed happen at oil–water interfaces,[21] but not at a liquid–air interface, the minimum known tension being reached with fluorinated liquids ($\sim$10 mN m^{-1}). Very few measurements of the surface pressure of particle-laden air–water surfaces have been reported to date; comparatively many more were performed at oil–water interfaces.[21,22] These measurements show that the surface tension is lower than that of water, but that it is non-zero ($\gamma \approx 30$ mN m^{-1}).[20]

A more elaborate theoretical description has recently been offered.[23] At equilibrium, small particles (smooth and much smaller than the capillary length, hence not sensitive to gravity) position themselves at the surface in order to achieve the equilibrium contact angle without distorting the surface. Upon compression, they close pack and since they are irreversibly adsorbed, the surface may be distorted, introducing a negative contribution to the surface energy that slows down coarsening.

It is in fact not necessary to create a distortion of the surface to suppress coarsening. Coarsening can also be stopped if the surface layer possesses a sufficiently large resistance to compression and is able to halt the shrinkage process of the small bubbles.[24] This resistance is quantified by an elastic compression modulus E, defined as (by analogy with the three-dimensional compression modulus $-V\mathrm{d}p/\mathrm{d}V$, logarithmic derivative of pressure p with respect to volume V):

$$E = -A\ \mathrm{d}\Pi/\mathrm{d}A = -\Gamma\ \mathrm{d}\gamma/\mathrm{d}\Gamma \qquad (3)$$

A being the surface area ($\Gamma \sim 1/A$). If this modulus is such that $E > \gamma/2$, coarsening is stopped. This simple condition can be obtained by writing that the pressure in the bubbles does not increase any more with decreasing radius:

$$\frac{d(\gamma/R)}{dR} = \frac{1}{R}\frac{d\gamma}{dR} - \frac{\gamma}{R^2} = \frac{1}{R^2}(2E - \gamma) > 0$$

In the case of surfactants, this condition is usually satisfied but the foam still coarsens. This is because, upon slow enough compression, the surfactant can desorb from the surface into the bulk, and the surface coverage is no longer inversely proportional to A: the apparent resistance to compression is much smaller than that estimated from eqn (3), valid only for fast compressions (or insoluble monolayers).

Our earlier surface pressure measurements performed on a Langmuir trough[20] allow us to estimate the compression modulus E for different particle surface concentrations. Here, eqn (3) can be used, because the particles are irreversibly adsorbed. E increases with surface concentration Γ and is maximum at Γ^* when the particles come into contact (jamming; above Γ^*, the layer becomes solid). $E = 80$ mN m^{-1} at Γ^*, whereas the surface tension is of the order of 30 mN m^{-1}.[20] One therefore has $E > \gamma/2$ in this case. For the surface concentration corresponding to the smaller bulk concentration, $C = 0.1$ wt%, the surface pressure is almost zero, $\gamma \sim \gamma_w \sim 72$ mN m^{-1} and $E \approx 0$, so that coarsening is not inhibited as in surfactant foams. This confirms that coarsening could be prevented near full surface coverage, because, unlike surfactant, the particles are irreversibly adsorbed.[4]

However, experiments on protein foams where the adsorption is also deemed irreversible and the compression moduli high, show that these foams coarsen. This was recently explained by the existence of a collapse of the surface layers: above full protein coverage, the protein monolayer can continue to be compressed forming multilayers.[25] The small bubbles can therefore continue to shrink, losing their spherical shape only when they are extremely small.[26] In this situation, coarsening can only be avoided if the surface layer δ is thick:[25] $\delta > 1.5R\gamma/E$. A suppression of this type has been seen in mini-emulsions stabilised by thick polymer layers.[27] However, in the particle-stabilised foams, bubbles are always much larger than surface layer thicknesses, and this mechanism is therefore unable to explain the absence of coarsening in such foams. So, the absence of coarsening could reflect the absence of collapse of the particle layers, at least for the conditions encountered on the bubble surfaces.

In surface pressure measurements carried out in a Langmuir trough using compression with barriers, the surface pressure saturates at large Γ ($\Gamma > \Gamma^*$), which can be seen as a signature of collapse. However, the measurement of surface tension is probably questionable when the layer becomes solid-like, and this saturation might be an artefact. Furthermore, optical observations of the particle layers showed that the layer buckles along lines parallel to the barriers.[20] On the other hand, the stress applied in the Langmuir trough (of the order of E/δ, δ being the layer thickness) is much larger than at the surface layers in the foam (of the order of E/R; the connections between foam films, or plateau borders, that are the curved surface portions in the foams, have dimensions of the order of $R\phi^{1/2} \sim R$ for the volume fractions used here). Let us also recall that the energy barrier for collapse is very large: about 3000 kT per particle is needed to pull them out of the interface. Moreover, it has been observed that when two bubbles covered by particle layers coalesce, after the film between them ruptures, the shape does not relax towards a single sphere in order to minimize the area. In contrast to the surfactant case, the bubble conserves an elongated shape.[28] This type of observation also proves that the surface area cannot decrease because collapse of the particle layers is prevented.

It should be mentioned that isolated particle-laden bubbles (with particle-to-bubble radius ratio of about 0.1) become faceted when the particles are forced into contact.[9] This of course reduces the pressure difference between the interior and the exterior. Bubble surfaces in foams already have flat portions –

those of films between bubbles (accounted for in eqn (2) by the parameter β that depends on curvature). It is, however, possible that the junctions between films (plateau borders) are also faceted, and that the coarsening rate is slower than the one given in eqn (2). Another possible contribution to the reduction of internal pressure is the buckling of the surface layers, which reduces the mean curvature, exactly as the liquid bridges between particles in the model of Kam and Rossen.[23]

5. Conclusion

In conclusion, we show that it is possible to produce large amounts of foam stabilized only by solid particles, that have controlled bubble size and that can last for months. This allowed us to perform a quantitative study of coarsening of particle-stabilised foams and to demonstrate that coarsening is blocked. With the help of independent studies of the particle layers, we have been able to correlate the interfacial properties and the macroscopic temporal evolution of the foam. Particle foams appear to be the only known foam system where coarsening could be inhibited by surface elasticity. We also show that a threshold in particle concentration can be observed, both in the microscopic and macroscopic behaviour. Below full bubble coverage, coarsening is not avoided and a particle-containing foam is destabilized as fast as a common surfactant foam. Further work is currently underway to better characterize the mechanical behaviour of the foam films to go further in the understanding of the collapse yield.

References

1 D. Weaire and S. Hutzler, *The Physics of Foams*, Oxford University Press, Oxford, 1999.
2 J. Banhart, *Adv. Eng. Mater.*, 2006, **8**, 781.
3 R. G. Alargova, D. S. Warhadpande, V. N. Paunov and O. D. Velev, *Langmuir*, 2004, **20**, 10371.
4 B. P. Binks and T. S. Horozov, *Angew. Chem., Int. Ed.*, 2005, **44**, 3722.
5 U. T. Gonzenbach, A. R. Studart, E. Tervoort and L. J. Gauckler, *Angew. Chem., Int. Ed.*, 2006, **45**, 3526.
6 S. Fujii, A. J. Ryan and S. P. Armes, *J. Am. Chem. Soc.*, 2006, **128**, 7882.
7 W. Ramsden, *Proc. R. Soc. A*, 1903, **72**, 156.
8 Z. Du, M. P. Bilbao-Montoya, B. P. Binks, E. Dickinson, R. Ettelaie and B. S. Murray, *Langmuir*, 2003, **19**, 3106.
9 M. Abkarian, A. B. Subramaniam, S.-H. Kim, R. J. Larsen, S.-M. Yang and H. A. Stone, *Phys. Rev. Lett.*, 2007, **99**, 188301.
10 A. M. Ganan-Calvo and J. M. Gordillo, *Phys. Rev. Lett.*, 2001, **87**, 274501; P. Garstecki, M. J. Fuerstman, H. A. Stone and G. M. Whitesides, *Lab Chip*, 2006, **6**, 437.
11 A. Saint Jalmes, M. U. Vera and D. J. Durian, *Eur. Phys. J. B*, 1999, **12**, 67.
12 A. Saint-Jalmes, M.-L. Peugeot, H. Ferraz and D. Langevin, *Colloids Surf., A*, 2005, **263**, 219.
13 M. U. Vera, A. Saint-Jalmes and D. J. Durian, *Appl. Opt.*, 2001, **40**, 4210.
14 W. W. Mullins, *J. Appl. Phys.*, 1986, **59**, 1341.
15 D. J. Durian, D. A. Weitz and D. J. Pine, *Phys. Rev. A*, 1991, **44**, 7902.
16 S. H. Hilgenfeldt, S. A. Koehler and H. A. Stone, *Phys. Rev. Lett.*, 2001, **86**, 4704.
17 S. Hilgenfeldt, A. M. Kraynik, S. A. Kohler and H. A. Stone, *Phys. Rev. Lett.*, 2001, **86**, 2685; S. Jurine, S. Cox and F. Graner, *Colloids Surf., A*, 2005, **263**, 18.
18 J. Lambert, I. Cantat, R. Mokso, P. Cloetens, J. Glazier and F. Graner, *Phys. Rev. Lett.*, 2007, **99**, 058304.
19 A. Saint Jalmes, in preparation.
20 M. Safouane, D. Langevin and B. P. Binks, *Langmuir*, 2007, **23**, 11546.
21 R. Aveyard, J. H. Clint, D. Nees and N. Quirke, *Langmuir*, 2000, **16**, 8820.
22 R. Aveyard, J. H. Clint, D. Nees and V. N. Paunov, *Langmuir*, 2000, **16**, 1969.
23 S. I. Kam and W. R. Rossen, *J. Colloid Interface Sci.*, 1999, **213**, 329.
24 J. Lucassen in Anionic Surfactants, *Surfactant Science Series*, vol. 11, ed. E. Lucassen-Reynders, Marcel Dekker, New York, 1981, p. 258.
25 M. B. J. Meinders and T. van Vliet, *Adv. Colloid Interface Sci.*, 2004, **108–109**, 119.
26 E. Dickinson, R. Ettelaie, B. S. Murray and Z. Du, *J. Colloid Interface Sci.*, 2002, **252**, 202.
27 S. Mun and D. J. McClements, *Langmuir*, 2006, **22**, 1551.
28 A. B. Subramaniam, M. Abkarian, L. Mahadevan and H. A. Stone, *Langmuir*, 2006, **22**, 10204.